Letter

Out-of-equilibrium response and fluctuation-dissipation violations across scales in flocking systems

Federica Ferretti,[1,*] Irene Giardina,[2,3,4,†] Tomas Grigera,[5,6,7,3] Giulia Pisegna,[8] and Mario Veca[2,‡]

[1]Department of Chemical Engineering, Massachusetts Institute of Technology, Cambridge, Massachusetts 02139, USA
[2]Dipartimento di Fisica, Università Sapienza, 00185 Rome, Italy
[3]Istituto Sistemi Complessi, Consiglio Nazionale delle Ricerche, UOS Sapienza, 00185 Rome, Italy
[4]INFN, Unità di Roma 1, 00185 Rome, Italy
[5]Instituto de Física de Líquidos y Sistemas Biológicos (IFLySiB), Universidad Nacional de La Plata and CONICET, La Plata, Argentina
[6]CCT CONICET La Plata, Consejo Nacional de Investigaciones Científicas y Técnicas, La Plata, Argentina
[7]Departamento de Física, Facultad de Ciencias Exactas, Universidad Nacional de La Plata, La Plata, Argentina
[8]Max Planck Institute for Dynamics and Self-Organization (MPI-DS), D-37077 Goettingen, Germany

(Received 6 June 2024; accepted 9 June 2025; published 7 July 2025)

Flocking systems are known to be strongly out of equilibrium. Energy input occurs at the individual level to ensure self-propulsion, and the individual motility, in turn, contributes to ordering, enhancing information propagation and strengthening collective motion. However, even beyond ordering, a crucial feature of natural aggregations is response. How, then, do off-equilibrium features affect the response of the system? In this work, we consider a minimal model of flocking and investigate response behavior under directional perturbations. We show that equilibrium dynamical fluctuation-dissipation relations between response and correlations are violated, both at the local and at the global levels. The amount of violation peaks at the ordering transition, exactly as for the entropy production rate. Entropy is always produced locally and connected to the local fluctuation-dissipation violation via Harada-Sasa relationships. However, cooperative mechanisms close to the transition spread off-equilibrium effects to the whole system, producing an out-of-equilibrium response on the global scale. Our findings elucidate the role of activity and interactions in the cost repartition of collective behavior and explain what is observed in experiments on natural living groups.

DOI: 10.1103/dg4n-1f4f

Introduction. Collective motion in living systems has been observed on different scales and regimes, from swimming bacteria and cell colonies to insect swarms and bird flocks [1]. From the perspective of statistical physics, these phenomena represent paradigmatic instances of nonequilibrium emergent behavior and they have been intensively studied in the context of active matter [2–4]. Broadly speaking, a flock has the following distinctive features: individuals are 'active', i.e., they are endowed with a self-propulsion mechanism transforming energy into motion, and they coordinate with each other via short-range interaction rules. The combination of motility and interactions leads to a nontrivial phenomenology comprising kinetic ordering transitions, novel classes of critical behavior and motility induced phase separation [5–8].

The impact of activity on order has been investigated at length [5,9,10]. On the other hand, much less is known on how nonequilibrium features affect the response of the system to perturbations. Response is a key trait for survival in living aggregations. Even more than order itself, it provides a *bona fide* signature of collective behavior, by quantifying the ability to retain global coherence in presence of external signals or threats. In this work, we systematically address this question. We consider an archetypal model of flocking and compute analytically and numerically the response function. We show that equilibrium dynamical fluctuation-dissipation relations between response and correlations are violated on all timescales, and we quantify the corresponding deviation across the phase diagram and across scales. Finally, we elucidate how interactions and motility affect the response, suggesting potential strategies for collective adaptation.

The model. We consider a continuous time generalization of the Vicsek model of flocking [5,11] where N self-propelled particles regulate their own speed using a speed control potential, and interact locally via velocity alignment [12,13]. The equations of motion are

$$\frac{d\mathbf{v}_i}{dt} = -\frac{\partial \mathcal{H}}{\partial \mathbf{v}_i} + \boldsymbol{\xi}_i, \quad \frac{d\mathbf{r}_i}{dt} = \mathbf{v}_i \,, \tag{1}$$

where $\boldsymbol{\xi}_i$ is a white noise with variance $\langle \xi_{i\alpha}(t)\xi_{j\beta}(t')\rangle = 2T\delta_{ij}\delta_{\alpha\beta}\delta(t-t')$, the 'temperature' T thereby describing the

*Present address: NSF-Simons National Institute for Theory and Mathematics in Biology, Chicago, IL 60611, USA.
†Contact author: irene.giardina@uniroma1.it
‡Contact author: mario.veca@uniroma1.it

strength of the stochastic force. The velocity potential $\mathcal{H}$ reads

$$\mathcal{H} = \frac{J}{2}\sum_{ij} n_{ij}(\mathbf{v}_i - \mathbf{v}_j)^2 + \frac{g}{2}\sum_i (|\mathbf{v}_i| - v_0)^2 \,. \qquad (2)$$

The first term in this expression describes mutual adjustment between velocity vectors, J being the scale of the interaction and $n_{ij}(t)$ the adjacency matrix. In the following, we will adopt a metric interaction rule, thereby, $n_{ij}(t) = 1$ if particles i and j at time t have mutual distance smaller than a fixed range $r_0 = 1$, and $n_{ij}(t) = 0$ otherwise. The second term in Eq. (2) is the speed control, setting the individual speeds close to a cruising reference value v_0, with fluctuations regulated by the parameter g [14]. With decreasing noise strength, model (1) exhibits a kinetic ordering transition to a state of collective motion, where the mean group velocity $\mathbf{V} = (1/N)\sum_i \mathbf{v}_i$ and the global degree of alignment—the polarization $\mathbf{\Phi} = (1/N)\sum_i \mathbf{v}_i/|\mathbf{v}_i|$—are different from zero (see Sec. I of the Supplemental Material (SM) [15]). The observed phenomenology belongs to the class of the Vicsek model [5]. However, we consider a continuous (rather than discrete) time evolution and fluctuating (rather than fixed) speeds. These features, besides being biologically more realistic, are greatly advantageous for analytic computations. As $g \to \infty$ the speed control becomes a sharp constraint, mimicking the fixed speed case.

Response functions and fluctuation-dissipation relations. Our aim is to investigate response behavior, and to understand how it relates to ordering and to the out-of-equilibrium features of the model. Response to specific factors in the ordered phase has been considered in [16–18]. Here, we wish to perform a systematic study under more general conditions. To do so, we consider a perturbation protocol where external fields are applied to the individual velocities, i.e., $\mathcal{H} \to \mathcal{H} - \sum_i \mathbf{h}_i \cdot \mathbf{v}_i$ [7,19–21]. The linear response functions can be defined in the usual way as $R_{ij}^{\alpha\beta}(t,s) = \delta\langle v_i^\alpha(t)\rangle_h/\delta h_j^\beta(s)|_{h=0}$ [22]. In equilibrium systems, such response functions are related to the velocity correlation functions $C_{ij}^{\alpha\beta}(t,s) = \langle v_i^\alpha(t) v_j^\beta(s)\rangle$ by the dynamical Fluctuation Dissipation Theorem (FDT) [23]. However, model (1) is intrinsically out of equilibrium due to the active nature of the particles, and we expect violations of such relationships. In the stationary state all functions depend on time differences. For the diagonal spatial components (the only ones that, for symmetry reasons, are nonzero in our case), we can then write (for $t > s$)

$$TR_{ij}^{\alpha\alpha}(t-s) = -\frac{dC_{ij}^{\alpha\alpha}(t-s)}{dt} - d_{ij}^{\alpha\alpha}(t-s), \qquad (3)$$

where $d_{ij}^{\alpha\alpha}$ measures the deviation from equilibrium.

In general, computing the full response tensor is a demanding task, as one needs to apply local fields and monitor reactions for all pairs of individuals. On the contrary, *global responses* are more easily accessible and statistically more reliable. Let us then consider the simpler setup where we apply a uniform field $h_i^\alpha(t) = h_\alpha(t)$ on the system and we measure how the global mean velocity $\mathbf{V}$ is affected by the perturbation. In this case, the global linear response is given by $R_{\alpha\alpha}(t-s) = \delta\langle V_\alpha(t)\rangle/\delta h_\alpha(s)|_{h=0} = (1/N)\sum_{ij} R_{ij}^{\alpha\alpha}(t-s)$, and the analog of Eq. (3) is

$$TR_{\alpha\alpha}(t-s) = -\frac{dC_{\alpha\alpha}(t-s)}{dt} - d_{\alpha\alpha}(t-s)\,, \qquad (4)$$

with $C_{\alpha\alpha}(t-s) = N\langle V_\alpha(t)V_\alpha(s)\rangle$ and $d_{\alpha\alpha}(t-s) = (1/N)\sum_{ij} d_{ij}^{\alpha\alpha}(t-s)$.

Interestingly, for Langevin dynamics the response functions can be explicitly computed starting from the equations of motion. To this task, it is convenient to introduce the Onsager-Machlup action [24] $S[\{\mathbf{v}_i, \mathbf{r}_i\}]$, defined by

$$\begin{aligned} &P[\{\mathbf{v}_i(t), \mathbf{r}_i(t)\}] \\ &= \frac{1}{\mathcal{N}} \exp\{-S[\{\mathbf{v}_i(t), \mathbf{r}_i(t)\}]\} \\ &= \left\langle \delta\left(\mathbf{v}_i(t) - \mathbf{v}_i(0) - \int_0^t dt'\,[-\partial\mathcal{H}/\partial\mathbf{v}_i + \boldsymbol{\xi}_i(t')]\right)\right\rangle , \end{aligned} \qquad (5)$$

where averages are performed over the trajectory realizations. In terms of the action S, the response functions can be written as $R_{ij}^{\alpha\alpha}(t,s) = -\langle v_i^\alpha(t)\ \delta S/\delta h_j^\alpha(s)\rangle|_{h=0}$. From Eq. (5) we get $S = (1/4T)\sum_{i,\alpha}\int_0^t dt'\ (\dot{v}_i^\alpha(t') + \partial\mathcal{H}/\partial v_i^\alpha(t'))^2$. Then, using standard techniques of stochastic calculus [22,25,26], one finds for $t > s$ (Sec. II of the SM [15]):

$$d_{\alpha\alpha} = \frac{gNv_0}{2}[\langle V_\alpha(t)\Phi_\alpha(s)\rangle - \langle V_\alpha(s)\Phi_\alpha(t)\rangle]\,. \qquad (6)$$

The deviation (6) has the time anti-symmetric form obtained in general for nonequilibrium Langevin equations (where it is called *asymmetry* [27,28]). Interestingly, in our case, it is expressed in terms of a particularly simple and accessible observable: the correlation between velocity and polarization, computed in zero field. Equation (6), therefore, allows to precisely quantify the FDT violation and to compute the response [via Eq. (4)] without actually perturbing the system.

FDT violations across the phase diagram. We now proceed to compute numerically the response functions and the deviations from equilibrium, and monitor them across the phase diagram of the model. We use a discretized version of Eq. (1) in $d = 3$, following a standard Euler integration scheme and working at fixed density $\rho = N/L^3$. We focus initially on checking the validity of Eq. (6). To do so, we compute the response in two ways, either perturbing the system or using Eqs. (4) and (6) in absence of perturbation. In fact, it is numerically more convenient to look at the integrated version of Eq. (4), i.e., $T\chi_{\alpha\alpha}(t) = [C_{\alpha\alpha}(0) - C_{\alpha\alpha}(t)] - D_{\alpha\alpha}(t)$, where $\chi_{\alpha\alpha}(t) = \int_0^t d\tau R_{\alpha\alpha}(\tau)$ is the integrated response [25] and $D_{\alpha\alpha}(t) = \int_0^t d\tau d_{\alpha\alpha}(\tau)$. For $T > T_c$ all coordinates α are statistically equivalent; for $T < T_c$ we consider the longitudinal component, i.e., we choose α as the direction of the polarization (see SM, Sec.I for details). The result is displayed in the inset of Fig. 1(b), where we can clearly see that the response curves obtained in the two ways coincide within statistical fluctuations. Once convinced that we can trust Eq. (6), we can then exploit this expression to compute the deviation function, and therefore the response, without actually perturbing the system. The deviation function $d(t)$ is displayed in Fig. 1(a) for several values of the temperature (we drop the coordinate index for notation convenience). In general, $d(t)$ shows a

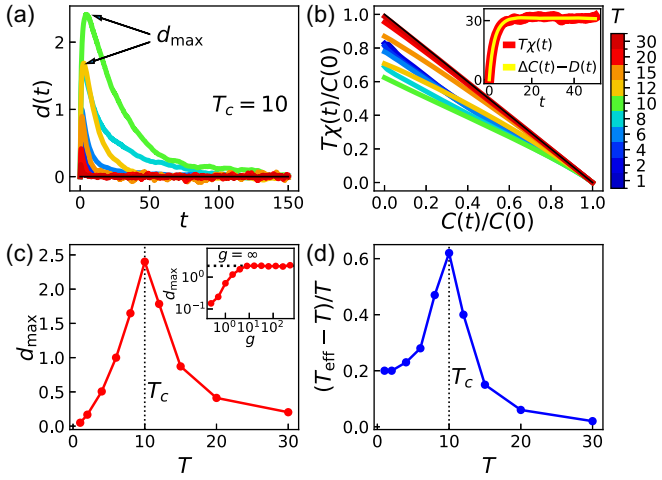

FIG. 1. FDT Violation. (a) Deviation $d(t)$ as a function of time for different temperatures. (b) Integrated response vs correlation for different temperatures; both quantities are normalized by $C(t = 0)$ and the black line corresponds to equilibrium. Inset: integrated response computed by perturbing the system (red) or by using Eqs. (6) and (4) (yellow), for $T = 15$. (c) Maximum of the deviation function d_{max} as a function of temperature. Inset: d_{max} as a function of g. (d) Asymptotic off-equilibrium offset $T_{eff}(\infty)/T - 1$ as a function of temperature. The parameters of the simulation are $J = 1.5$, $v_0 = 4$, $g = 4$, $\rho = 0.25$, $N = 512$, with temperatures described by the color bar and $T_c = 10$ (light green).

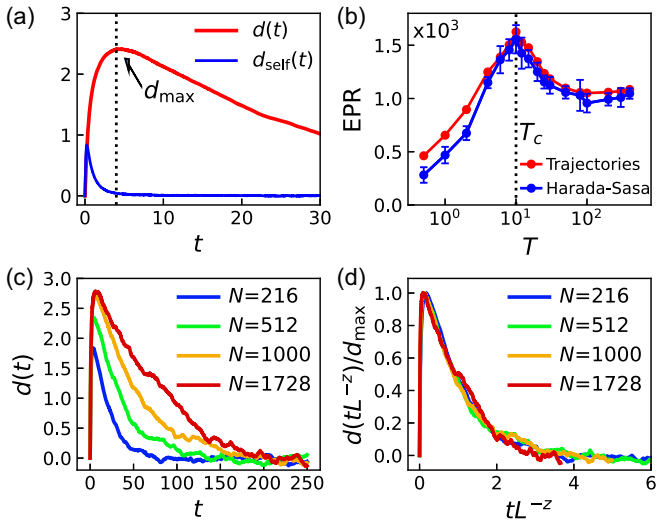

FIG. 2. FDT violations across scales. (a) Self-contribution d_{self} (blue curve) and full deviation (red curve) as a function of time at $T = T_c$. (b) EPR computed using the trajectories with Eq. (7) (red points) and the Harada-Sasa formula (blue points). (c) Deviation curves $d(t)$ at $T = T_c$ for several system sizes. For each value of N, T_c is computed as the temperature where the fluctuations of the polarization are maximal (see SM). (d) Rescaled deviation $d(t)/d_{max}(N)$ as a function of the rescaled time tL^{-z}, with $z = 1.7$. The parameters of the simulation are $J = 1.5$, $v_0 = 4$, $g = 4$, $\rho = 0.25$. In panels (a) and (b) $N = 512$. Results at $\rho = 1.5$ can be found in the SM.

first quick increase on short timescales towards a maximum, and a slower decay to zero at longer times. We immediately notice that the violation is larger and more extended in time as the temperature approaches the critical value T_c of the kinetic transition. A different way—which is standard in the literature—to capture out-of-equilibrium behavior is to plot the integrated response parametrically as a function of the correlation function [29]. In equilibrium dynamics the expected behavior is a straight line with slope given by (minus) the inverse temperature. On the contrary, as shown in Fig. 1(b), in our model the curves clearly depart from the equilibrium one, and such departure looks more pronounced close to criticality, consistently with Fig. 1(a).

To better investigate the role of temperature, we now introduce two synthetic quantifiers of the departure from equilibrium. As a first measure, we consider the maximum d_{max} of the deviation function $d(t)$, which occurs on short timescales. In Fig. 1(c) d_{max} is plotted as a function of temperature, and it displays a sharp maximum at the transition temperature. In the inset, we also show $d_{max}(T_c)$ as a function of g: it quickly converges to a well-defined $g \to \infty$ asymptotic value, showing that equilibrium violations persist and are well-captured also in the fixed speed limit (see Sec. V of the SM for more discussion).

Another quantity that is widely used in the literature to quantify FDT violations is the so-called *effective temperature* [25,30,31], defined as the ratio between the correlation and the integrated response $T_{eff}(t) = (C(0) - C(t))/\chi(t)$ [32]. In Fig. 1(d), we display the asymptotic value $(T_{eff}(t \to \infty) - T)/T$ (which is zero at equilibrium) as a function of temperature. Also this quantity—which encodes FDT violations on long timescales—displays a maximum in correspondence of the critical temperature.

FDT violations across scales. The above results indicate that FDT violations are maximal at the transition, and that the response is strongly out of equilibrium on all time-scales. The behavior in time of the deviation function $d(t)$, however, suggests that different processes might regulate the short time regime and the long time decay. In Fig. 2(a) we plot the self contribution $d_{self} = (1/N)\sum_i d_{ii}$ to the deviation and compare it to the full function. d_{self} can be computed by evaluating the responses $R^{\alpha\alpha}_{ii}$ via Mallivian weight sampling [33] (see SM) and deriving d_{ii} from Eq. (3). This contribution dominates the first regime of $d(t)$ and it decays to zero on a timescale corresponding to the location of d_{max}.

Interestingly, d_{self} is connected to another quantifier of nonequilibrium, the Entropy Production Rate (EPR), which measures the amount of violation of detailed balance in the system due to positional rearrangements [34]. The entropy production is defined as the logarithm of the ratio between the probability of a forward and a backward trajectory [35,36], and it can be computed from the Onsager-Machlup action [see Eq. (5)]. For the EPR, in the stationary state, we get (see Sec. III of the SM [15])

$$\mathrm{EPR} = \lim_{\tau\to\infty} \frac{1}{\tau}\left\langle \frac{J}{2T}\int_0^\tau d\tau \sum_{ij} \frac{dn_{ij}}{dt} \circ \sum_\alpha \left(v_i^\alpha - v_j^\alpha\right)^2 \right\rangle, \tag{7}$$

where $\circ$ denotes the Stratonovitch prescription. A discretized version of this expression can be used to evaluate the EPR from numerical trajectories. The result is displayed in

Fig. 2(b) and it shows that the EPR also peaks at the critical temperature [37,38]. In fact, the EPR and some FDT violations are directly related to each other via Harada-Sasa relationships [39], which we explicitly derive in Sec. IV of the SM [15],

$$\mathrm{EPR} = \sum_{i,\alpha} \int \frac{d\omega}{2\pi} \frac{\omega}{T} \left[\omega \tilde{C}^{\alpha\alpha}_{ii}(\omega) - 2T\, \mathrm{Im}(\tilde{R}^{\alpha\alpha}_{ii}(\omega)) \right] = \frac{N}{T} \frac{d}{dt} \left(\sum_{\alpha} d^{\alpha\alpha}_{\mathrm{self}}(t) \right) \Big|_{t=0^+} \tag{8}$$

We have verified this relation, by computing the EPR via the integral in Eq. (8) and comparing the result with Eq. (7), see Fig. 2(b) and Sec. IV of the SM [15].

The connection with the EPR helps understanding the origin of the short time regime of the FDT violation: it is directly determined by the production of entropy in the system. Equation (7) shows that the EPR depends on the rate of change of the interaction network dn_{ij}/dt, that is on how quickly nearby particles enter and exit their interaction range. It is, therefore, a local process. Besides, since mutual diffusion in space is maximal at the transition [37,40,41] the EPR peaks at $T = T_c$ [42].

As we already noticed, strong deviations from equilibrium are observed in the response also on the long timescales, as testified by the slow decay of the function $d(t)$ and by the behavior of $T_{\mathrm{eff}}(t = \infty)$ across the phase diagram [see Fig. 1(d)]. To explain this behavior, it is crucial to consider the interacting nature of the system and, in particular, the occurrence of strong cooperative phenomena as the transition point is approached. At large times, the deviation function is dominated by the non-self-contribution, and it therefore involves correlations between pairs of particles. Close to T_c, such correlations become long range, distributing off-equilibrium effects to the large scales and slowing down the decay of $d(t)$.

To confirm the collective nature of FDT violations at large times, we performed simulations for systems with different values of N, at the critical temperature. The resulting $d(t)$ curves are displayed in Fig. 2(c): the short time increase of the deviation function, being related to a local process, is always the same; on the contrary, the long time decay is slower the larger the system, a behavior typical of critical slowing down. Indeed, we show in Fig. 2(d) that the deviation curves obey dynamic scaling, falling one on top of the other once the time is rescaled by a characteristic time growing with the system's size as L^z. The value of the dynamic exponent used for the collapse is $z = 1.7$, that is the value predicted by the incompressible field theory of the Vicsek model [43]. We conclude that—as long as the system is homogeneous enough in density and the incompressible regime holds [44]—long time FDT violations are a critical effect. Above a (density-dependent) crossover size, the cooperative processes at the transition are dominated by heterogeneities [7,44] and we expect the long time dynamics to be ruled by different laws. The simulations performed in this paper, as well as experiments on natural groups in $d = 3$ [45,46], all belong to the incompressible regime (see Sec. I of the SM [15]).

The general picture can be summarized as follows. Energy is injected in the system at the individual level via the particle self-propulsion and the relative speed control function. Then, entropy is produced locally, every time two particles start/stop interacting with each other, and it is maximal at T_c due to the fast network reshuffling. Violations of detailed balance immediately alter FDT relations on the short scales. The existence of long-range cooperative processes close to the transition then propagate off-equilibrium effects through the whole system. FDT deviations therefore persist at large times, and their overall amount peaks at the transition point.

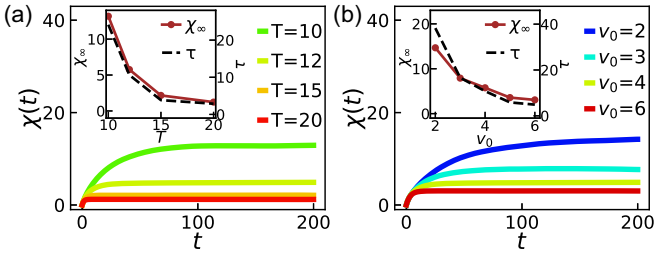

FIG. 3. (a) Integrated response at different temperatures, for $v_0 = 4$. Inset: relaxation time (computed as in [47]) and asymptotic response vs T ($T_c = 10$). (b) Integrated response for different motilities v_0. The temperature is set so that $T/T_c(v_0) - 1 = 0.2$. Inset: relaxation time and asymptotic response vs v_0. All other parameters as in Fig. 1.

Response control: accuracy vs activity. What are the consequences of the above scenario on the global response of the system? As illustrated in Fig. 3(a), the response exhibits the dynamical slowing down typical of second-order phase transitions, the system taking longer to react as $T \to T_c$. The proximity to the critical point is, therefore, a major factor regulating response behavior. An important additional ingredient is related to the out-of-equilibrium nature of the system, which—as we have seen—manifests on all timescales. Since the deviation function contributes with a negative sign to the response [see Eq. (4)], we expect a stronger activity to produce a smaller response. To investigate this point, we performed numerical simulations for different values of the motility v_0. To disentangle the role of activity from critical effects for any given v_0, we computed the transition point $T_c(v_0)$ and considered the system at the same relative distance from it (see SM). The behavior of the integrated response is displayed in Fig. 3(b) and it shows that, indeed, the larger the motility, the smaller the full-response curve. When increasing v_0, the response relaxes more quickly and its asymptotic value $\chi(\infty)$ decreases (see Fig. 3 inset). Overall, these results suggest possible adaptive strategies where—by tuning the accuracy of mutual alignment (i.e., T vs J) or the value of the cruising speed (v_0)—a system can privilege either the strength or the rapidity of its global response. A decreased intensity of the response makes the collective state more resilient against external perturbations. Concurrently, a swifter relaxation allows adjusting more promptly. Different contexts might benefit from robustness or sensitivity, making a flexible response an important asset for survival.

Conclusions. The way a system manages its energy budget is a crucial issue for living systems, which typically acquire external resources to build functional ordered structures and dissipate excess entropy in the environment. Understanding

how this occurs and what determines the repartition of this process is, therefore, an important question [48–53]. Indeed, it remains, in general, unclear whether activity in the individuals of an aggregation affects the dynamics also at the macroscopic level [54–58]. Our results show that, in fact, in flocking systems, nonequilibrium features do manifest on all scales, being stronger on the short times and slowly decaying at long ones. The key ingredient for this to occur is the combination of the individual driving enforcing self-propulsion and the presence of an ordering transition coupling dynamical modes over the whole system.

Finally, we note that our results explain what is observed in experiments on natural groups. In flocks of birds the network changes very slowly [59] and the collective turns they exhibit can be quantitatively described using equilibriumlike theories [60]. In swarms of midges, on the other hand, network rearrangements are much quicker and out-of-equilibrium features must be taken into account to reproduce the measured dynamical observables [46]. This is consistent with our findings: flocks are highly polarized groups and therefore belong to a region where both EPR and FDT violations are small (see Fig. 1); swarms, on the contrary, are quasi-critical systems and obey dynamic scaling [61,62], thereby representing instances at the peak of the violation-noise diagram.

Acknowledgments. We thank A. Cavagna, J. Cristín and G. Fausti for many interesting discussions. This work was supported by MIUR (Grant No. PRIN-2020PFCXPE) and by ERC RG.BIO (Grant No. 785932).

[1] J. Krause and G. D. Ruxton, *Living in Groups* (Oxford University Press, Oxford, 2002).

[2] M. C. Marchetti, J. F. Joanny, S. Ramaswamy, T. B. Liverpool, J. Prost, M. Rao, and R. A. Simha, Hydrodynamics of soft active matter, Rev. Mod. Phys. **85**, 1143 (2013).

[3] S. Ramaswamy, The mechanics and statistics of active matter, Annu. Rev. Condens. Matter Phys. **1**, 323 (2010).

[4] G. Gompper, R. G. Winkler, T. Speck, A. Solon, C. Nardini, F. Peruani, H. Löwen, R. Golestanian, U. B. Kaupp, L. Alvarez *et al.*, The 2020 motile active matter roadmap, J. Phys.: Condens. Matter **32**, 193001 (2020).

[5] T. Vicsek, A. Czirók, E. Ben-Jacob, I. Cohen, and O. Shochet, Novel type of phase transition in a system of self-driven particles, Phys. Rev. Lett. **75**, 1226 (1995).

[6] T. Vicsek and A. Zafeiris, Collective motion, Phys. Rep. **517**, 71 (2012).

[7] H. Chaté, F. Ginelli, G. Grégoire, and F. Raynaud, Collective motion of self-propelled particles interacting without cohesion, Phys. Rev. E **77**, 046113 (2008).

[8] M. E. Cates and J. Tailleur, Motility-induced phase separation, Annu. Rev. Condens. Matter Phys. **6**, 219 (2015).

[9] J. Toner and Y. Tu, Long-range order in a two-dimensional dynamical XY model: How birds fly together, Phys. Rev. Lett. **75**, 4326 (1995).

[10] J. Toner and Y. Tu, Flocks, herds, and schools: A quantitative theory of flocking, Phys. Rev. E **58**, 4828 (1998).

[11] O. Chepizhko, D. Saintillan, and F. Peruani, Revisiting the emergence of order in active matter, Soft Matter **17**, 3113 (2021).

[12] W. Bialek, A. Cavagna, I. Giardina, T. Mora, O. Pohl, E. Silvestri, M. Viale, and A. M. Walczak, Social interactions dominate speed control in poising natural flocks near criticality, Proc. Natl. Acad. Sci. **111**, 7212 (2014).

[13] A. Cavagna, A. Culla, X. Feng, I. Giardina, T. S. Grigera, W. Kion-Crosby, S. Melillo, G. Pisegna, L. Postiglione, and P. Villegas, Marginal speed confinement resolves the conflict between correlation and control in collective behaviour, Nat. Commun. **13**, 2315 (2022).

[14] We could have chosen different forms for the speed potential (e.g., functions of $\mathbf{v}_i^2$ rather than of $|\mathbf{v}_i|$). In the region around the ordering transition—which is the most interesting regime for our analysis—there is not much difference, so we stick to the simple Gaussian shape of Eq. (2).

[15] See Supplemental Material at http://link.aps.org/supplemental/10.1103/dg4n-1f4f for more details on the numerical simulations, including the phase diagram, finite size scaling, dynamic scaling, and results for different values of density and motility (Sec. I); a step-by-step derivation of the response function and of Eq. (6) (Sec. II); a full derivation of the entropy production rate from Eq. (7) and the Harada-Sasa relationship of Eq. (8) (Secs. III and IV); and a discussion of the equilibrium limits (Sec. V). The Supplemental Material also contains Refs. [63–72].

[16] A. Cavagna, L. Del Castello, I. Giardina, T. Grigera, A. Jelic, S. Melillo, T. Mora, L. Parisi, E. Silvestri, M. Viale *et al.*, Flocking and turning: A new model for self-organized collective motion, J. Stat. Phys. **158**, 601 (2015).

[17] D. J. Pearce and L. Giomi, Linear response to leadership, effective temperature, and decision making in flocks, Phys. Rev. E **94**, 022612 (2016).

[18] D. Geiß, K. Kroy, and V. Holubec, Information conduction and convection in noiseless Vicsek flocks, Phys. Rev. E **106**, 014609 (2022).

[19] N. Kyriakopoulos, F. Ginelli, and J. Toner, Leading birds by their beaks: The response of flocks to external perturbations, New J. Phys. **18**, 073039 (2016).

[20] M. Brambati, G. Fava, and F. Ginelli, Signatures of directed and spontaneous flocking, Phys. Rev. E **106**, 024608 (2022).

[21] E. Loffredo, D. Venturelli, and I. Giardina, Collective response to local perturbations: How to evade threats without losing coherence, Phys. Biol. **20**, 035003 (2023).

[22] U. M. B. Marconi, A. Puglisi, L. Rondoni, and A. Vulpiani, Fluctuation–dissipation: Response theory in statistical physics, Phys. Rep. **461**, 111 (2008).

[23] R. Kubo, The fluctuation-dissipation theorem, Rep. Prog. Phys. **29**, 255 (1966).

[24] L. Onsager and S. Machlup, Fluctuations and irreversible processes, Phys. Rev. **91**, 1505 (1953).

[25] L. F. Cugliandolo, The effective temperature, J. Phys. A: Math. Theor. **44**, 483001 (2011).

[26] L. Caprini, Generalized fluctuation–dissipation relations holding in non-equilibrium dynamics, J. Stat. Mech. (2021) 063202.

[27] L. F. Cugliandolo, J. Kurchan, and G. Parisi, Off equilibrium dynamics and aging in unfrustrated systems, J. Phys. I **4**, 1641 (1994).

[28] M. Baiesi, C. Maes, and B. Wynants, Fluctuations and response of nonequilibrium states, Phys. Rev. Lett. **103**, 010602 (2009).

[29] J.-P. Bouchaud, L. Cugliandolo, J. Kurchan, and M. Mézard, Spin glasses and random fields, Directions in Condensed Matter Phy. **12**, 443 (1998).

[30] P. Hohenberg and B. I. Shraiman, Chaotic behavior of an extended system, Physica D **37**, 109 (1989).

[31] L. F. Cugliandolo, J. Kurchan, and L. Peliti, Energy flow, partial equilibration, and effective temperatures in systems with slow dynamics, Phys. Rev. E **55**, 3898 (1997).

[32] Even though T_{eff} represents a real temperature only in a few cases, we will stick for convenience to this terminology.

[33] P. B. Warren and R. J. Allen, Malliavin weight sampling for computing sensitivity coefficients in Brownian dynamics simulations, Phys. Rev. Lett. **109**, 250601 (2012).

[34] The entropy production considered here, as in previous works on flocking [37,38], is a statistical measure of time-reversal asymmetry in position space and it represents only a lower bound to the full energy dissipation of animals in a flock, which also includes inaccessible internal degrees of freedom [73].

[35] U. Seifert, Stochastic thermodynamics, fluctuation theorems and molecular machines, Rep. Prog. Phys. **75**, 126001 (2012).

[36] F. Ritort, Nonequilibrium fluctuations in small systems: From physics to biology, Adv. Chem. Phys. **137**, 31 (2008).

[37] F. Ferretti, S. Grosse-Holz, C. Holmes, J. L. Shivers, I. Giardina, T. Mora, and A. M. Walczak, Signatures of irreversibility in microscopic models of flocking, Phys. Rev. E **106**, 034608 (2022).

[38] Q. Yu and Y. Tu, Energy cost for flocking of active spins: The cusped dissipation maximum at the flocking transition, Phys. Rev. Lett. **129**, 278001 (2022).

[39] T. Harada and S.-i. Sasa, Equality connecting energy dissipation with a violation of the fluctuation-response relation, Phys. Rev. Lett. **95**, 130602 (2005).

[40] Y. Tu, J. Toner, and M. Ulm, Sound waves and the absence of galilean invariance in flocks, Phys. Rev. Lett. **80**, 4819 (1998).

[41] H. Chaté, F. Ginelli, G. Grégoire, F. Peruani, and F. Raynaud, Modeling collective motion: Variations on the Vicsek model, Eur. Phys. J. B **64**, 451 (2008).

[42] At least for not-too-small values of g. We remind that g regulates the amplitude of speed fluctuations. If it is too small, speeds are not confined and they can alter the scenario so far described. This is, however, an unrealistic regime, as discussed at length in [13] in the case of natural flocks, which is not of interest to our analysis.

[43] L. Chen, J. Toner, and C. F. Lee, Critical phenomenon of the order–disorder transition in incompressible active fluids, New J. Phys. **17**, 042002 (2015).

[44] L. Di Carlo and M. Scandolo, Evidence of fluctuation-induced first-order phase transition in active matter, New J. Phys. **24**, 123032 (2022).

[45] A. Cavagna, A. Cimarelli, I. Giardina, A. Orlandi, G. Parisi, A. Procaccini, R. Santagati, and F. Stefanini, New statistical tools for analyzing the structure of animal groups, Math. Biosci. **214**, 32 (2008).

[46] A. Cavagna, L. Di Carlo, I. Giardina, T. S. Grigera, S. Melillo, L. Parisi, G. Pisegna, and M. Scandolo, Natural swarms in 3.99 dimensions, Nat. Phys. **19**, 1043 (2023).

[47] B. I. Halperin and P. C. Hohenberg, Scaling laws for dynamic critical phenomena, Phys. Rev. **177**, 952 (1969).

[48] F. S. Gnesotto, F. Mura, J. Gladrow, and C. P. Broedersz, Broken detailed balance and non-equilibrium dynamics in living systems: A review, Rep. Prog. Phys. **81**, 066601 (2018).

[49] C. W. Lynn, C. M. Holmes, W. Bialek, and D. J. Schwab, Decomposing the local arrow of time in interacting systems, Phys. Rev. Lett. **129**, 118101 (2022).

[50] E. Fodor, C. Nardini, M. E. Cates, J. Tailleur, P. Visco, and F. van Wijland, How far from equilibrium is active matter? Phys. Rev. Lett. **117**, 038103 (2016).

[51] A. Crisanti, A. Puglisi, and D. Villamaina, Nonequilibrium and information: The role of cross correlations, Phys. Rev. E **85**, 061127 (2012).

[52] M. Esposito, Stochastic thermodynamics under coarse graining, Phys. Rev. E **85**, 041125 (2012).

[53] Q. Yu, D. Zhang, and Y. Tu, Inverse power law scaling of energy dissipation rate in nonequilibrium reaction networks, Phys. Rev. Lett. **126**, 080601 (2021).

[54] D. A. Egolf, Equilibrium regained: From nonequilibrium chaos to statistical mechanics, Science **287**, 101 (2000).

[55] P.-S. Shim, H.-M. Chun, and J. D. Noh, Macroscopic time-reversal symmetry breaking at a nonequilibrium phase transition, Phys. Rev. E **93**, 012113 (2016).

[56] C. Nardini, É. Fodor, E. Tjhung, F. Van Wijland, J. Tailleur, and M. E. Cates, Entropy production in field theories without time-reversal symmetry: Quantifying the non-equilibrium character of active matter, Phys. Rev. X **7**, 021007 (2017).

[57] C. Maggi, N. Gnan, M. Paoluzzi, E. Zaccarelli, and A. Crisanti, Critical active dynamics is captured by a colored-noise driven field theory, Commun. Phys. **5**, 55 (2022).

[58] Ø. L. Borthne, E. Fodor, and M. E. Cates, Time-reversal symmetry violations and entropy production in field theories of polar active matter, New J. Phys. **22**, 123012 (2020).

[59] T. Mora, A. M. Walczak, L. Del Castello, F. Ginelli, S. Melillo, L. Parisi, M. Viale, A. Cavagna, and I. Giardina, Local equilibrium in bird flocks, Nat. Phys. **12**, 1153 (2016).

[60] A. Attanasi, A. Cavagna, L. Del Castello, I. Giardina, T. S. Grigera, A. Jelić, S. Melillo, L. Parisi, O. Pohl, E. Shen, and M. Viale, Information transfer and behavioural inertia in starling flocks, Nat. Phys. **10**, 691 (2014).

[61] A. Attanasi, A. Cavagna, L. Del Castello, I. Giardina, S. Melillo, L. Parisi, O. Pohl, B. Rossaro, E. Shen, E. Silvestri, and M. Viale, Finite-size scaling as a way to probe near-criticality in natural swarms, Phys. Rev. Lett. **113**, 238102 (2014).

[62] A. Cavagna, D. Conti, C. Creato, L. Del Castello, I. Giardina, T. S. Grigera, S. Melillo, L. Parisi, and M. Viale, Dynamic scaling in natural swarms, Nat. Phys. **13**, 914 (2017).

[63] V. Privman, *Finite Size Scaling and Numerical Simulation of Statistical Systems* (World Scientific, Singapore, 1990).

[64] D. J. Amit and V. Martin-Mayor, *Field Theory, the Renormalization Group, and Critical Phenomena: Graphs to Computers* (World Scientific Publishing Company, Singapore, 2005).

[65] G. Baglietto and E. V. Albano, Finite-size scaling analysis and dynamic study of the critical behavior of a model for the collec-

tive displacement of self-driven individuals, Phys. Rev. E **78**, 021125 (2008).

[66] E. Brézin and D. Wallace, Critical behavior of a classical heisenberg ferromagnet with many degrees of freedom, Phys. Rev. B **7**, 1967 (1973).

[67] E. Brézin, D. Wallace, and K. G. Wilson, Feynman-graph expansion for the equation of state near the critical point, Phys. Rev. B **7**, 232 (1973).

[68] L. P. Fischer, P. Pietzonka, and U. Seifert, Large deviation function for a driven underdamped particle in a periodic potential, Phys. Rev. E **97**, 022143 (2018).

[69] P. B. Warren and R. J. Allen, Malliavin weight sampling: A practical guide, Entropy **16**, 221 (2013).

[70] A. Cavagna, I. Giardina, F. Ginelli, T. Mora, D. Piovani, R. Tavarone, and A. M. Walczak, Dynamical maximum entropy approach to flocking, Phys. Rev. E **89**, 042707 (2014).

[71] T. Speck and U. Seifert, Restoring a fluctuation-dissipation theorem in a nonequilibrium steady state, Europhys. Lett. **74**, 391 (2006).

[72] R. Chetrite, G. Falkovich, and K. Gawedzki, Fluctuation relations in simple examples of non-equilibrium steady states, J. Stat. Mech. (2008) P08005.

[73] G. Falasco and M. Esposito, Macroscopic stochastic thermodynamics, Rev. Mod. Phys. **97**, 015002 (2025).